ELECTRONICS, TRIGGERING, AND DATA ACQUISITION FOR THE SSC

T. J. Devlin
Department of Physics and Astronomy, Rutgers - The State University
P. O. Box 849, Piscataway, NJ 08854

A. Lankford
Stanford Linear Accelerator Center
P. O. Box 4349, Stanford, CA 94305

H. H. Williams
Physics Department, University of Pennsylvania
Philadelphia, PA 19104

* * *

Participants in the Triggering and Electronics Group
Snowmass-86

Maris Abolins	*Michigan State University*
Richard Gustafson	*University of Michigan*
Marvin Johnson	*Fermilab*
Kunitaki Kondo	*University of Tsukuba*
Allen Odian	*Stanford Linear Accel. Center*
Lawrence Price	*Argonne National Laboratory*
Richard Van Berg	*University of Pennsylvania*
Yasuo Arai	*KEK - Natl. Lab for HEP*
Don Hartill	*Cornell University*
Stuart Kleinfelder	*Lawrence Berkeley Laboratory*
Takahiko Kondo	*KEK - Natl. Lab for HEP*
Takashi Ohsugi	*Hiroshima University*
Sergio Rescia	*Brookhaven National Laboratory*

SUMMARY

The main thrust of the Electronics and Triggering Group during the Snowmass-86 Summer Study was the development of plausible schemes for front- end electronics for calorimetry and central tracking in a "generic" 4π, detector. Solutions for a zero deadtime system appear to exist within the limitations of present technology. These involve fast pulse shaping to minimize the effects of pileup and analog storage of all information during 0.5 – 1μsec. for Level 1 trigger processing. An aggressive research and development program will be required if one is to fully exploit the capabilities of existing technology on the appropriate time scale.

INTRODUCTION

If experiments at the proposed Superconducting Super Collider (SSC) are to exploit adequately the full luminosity available, a major development of electronics will be required: this follows from the necessity of *simultaneously* satisfying the goals of high speed, low noise, and low power. The performance required, and the problems encountered, will be similar for many different types of experiments whether they utilize large 4π detectors, forward spectrometers, or other specialized detectors For the purposes of the present discussion, we will concentrate on the systems required for large 4π detectors since it is for this application that some of the problems are most acute.

The detector which we consider is discussed in detail in the Summary of the Detector Group[1] and in the reports of the individual subgroups[2–6]; a schematic diagram is presented in Figure 1. Here we simply note that it includes calorimetry, tracking systems, electron identification, and muon systems over approximately 5 units of rapidity. Further details which are relevant to the electronics are given in the discussion below. It is worth noting at this point, however, that each of the above systems will include 100,000 - 200,000 channels of electronics. We also note that nearly any type of detector will include calorimeter and tracking systems similar to those discussed here so that the conclusions concerning the electronics should be quite general

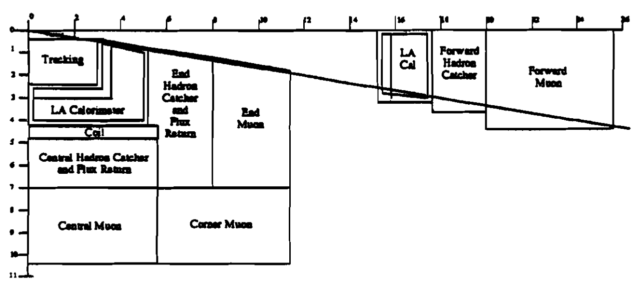

Figure 1
A schematic diagram of the 4π detector used as a model for the discussion of triggering and electronics.

Figure 2 presents a conceptual design for the overall system of electronics, triggering. and data acquisition. The major considerations that lead to this design, which is a natural evolution of existing systems, include the following:

(1) High luminosity, corresponding to an interaction rate of order 10^8 events per second. is essential if one is to be sensitive to many of the processes of greatest interest.

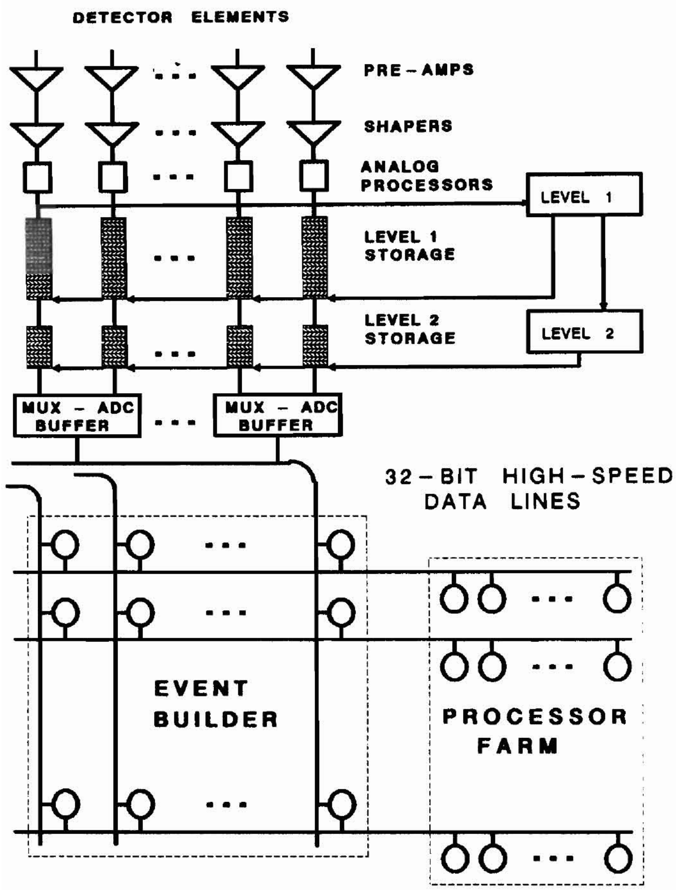

Figure 2
Schematic diagram showing the front end electronics, Level 1 Level 2 buffers (primarily analog) multiplexer - ADC - digital buffer, event builder, and processor farm.

(2) Both the high data rate and the complicated nature of the events require that each system be very finely segmented. Thus the tracking, calorimetry, muon identification systems, etc will each require of order 100,000 - 200,000 channels. For at least the calorimetry and tracking systems, the electronics must be low noise, fast, and low power.

(3) It does not seem to be feasible to form a trigger with significant rejection within the 16 nsec between beam crossings. Rather, estimates indicate that of order 500 - 1000 nsec will be required to form the initial, or Level 1, triggers. It will therefore be necessary to delay, or *pipeline*, all information from the detectors. Information crucial to further triggers is digitized during the Level 1 trigger processing.

(4) Following the inital trigger system which will pass events at a rate of $10^4 - 10^5$ per second, a second, *Level 2* trigger system, utilizing primarily special purpose hardware processors, will achieve a further rejection of events of approximately 100:1. Events passing the Level 1 system should be buffered so that fluctuations in the inital pass rate do not lead to deadtime and loss of efficiency. For events passing the Level 2 system, a matrix of scanners and ADC's will digitize the data for all channels containing information relevant to that event.

(5) Finally, a third Level of decision-making will be performed using general purpose processors capable of reasonably complete and sophisticated reconstruction of events.

The general flow of the electronics summarized in Figure 2 has been discussed in several previous workshops[7-12]. In addition, it is to a large extent modeled after existing experiments such as UA1 UA2, CDF, and D0. It is encouraging to note that the performance required at each stage has been obtained, or is likely to be obtained, in existing experiments. Thus, for example, UA1 and UA2 have obtained rejections exceeding 1000 in the equivalent of a Level 1 system for triggers on electrons, muons, and jets. CDF fully anticipates that its Level 2 and Level 3 system will achieve a combined rejection exceeding 10^4. That the total rejection of nearly 10^8 may be obtained remains to be demonstrated, however, since the selection criteria of the UA1-UA2 "Level 1" systems are strongly correlated with those planned for Level 2 - Level 3 in CDF. For one process of great interest, $H \rightarrow W^+W^-$ a study indicated that it should be feasible to attain the desired factor.[13] For many of the other processes of interest, further work clearly needs to be performed.

While all aspects of the electronics, trigger, and data acquisition system require significant development, it is evident that the most serious technological challenges involve the front end electronics. Also, the design of the preamplifiers, amplifiers, etc., is very closely linked with the design of the detectors. In fact, at the present time one can state without exaggeration that whether or not it is *possible* to build a detector with the desired characteristics depends in large measure on whether certain goals for the electronics can be achieved. For these reasons, and also because an earlier workshop at Fermilab[8] concentrated on triggering and data acquisition, it was decided to focus attention during the present workshop primarily on the front end electronics.

There will of course exist many different types of front end systems, including among others those for tracking, calorimetry, muon detection, transition radiation detectors, etc. Even within one of the above categories there exist multiple possibilities depending on whether one wishes to measure charge or time and on what resolution is required. It was decided to concentrate on tracking and calorimetry both because these systems are in a sense the most basic and also because it was felt that solutions to problems in these areas would very likely be applicable to systems for other detectors.

As background for its discussions, and also to provide inspiration, the group heard talks presented by a number of experts in the field. The speakers and topics presented included:

V. Radeka	Detector signal formation, noise properties, charge amplifiers, filtering, position sensing, and fast pulse shaping for tracking and calorimeter systems.
P. F. Manfredi	Semiconductor devices
S. Rescia	Fast pulse shaping for liquid argon calorimeters
D. Hartill	System design and reliability
J. Cresswell	GaAs CCD's
W. Smith	Calorimeter Electronics for ZEUS (HERA)
E. Elsen	Flash ADC's for drift chambers
H. Spieler	Monolithic preamplifiers, pixel detectors
M. Johnson	D0 Calorimeter electronics
E. Heijne	Microdetectors and microelectronics at CERN

P. Rehak	Fast pulse shaping for wire chambers, silicon drift detectors
S. Kleinfelder	Monolithic charge preamplifier
T. Kondo	Monolithic preamplifier for the Venus drift chamber

CALORIMETER ELECTRONICS

Introduction

To extract the optimal performance from a detector, the design of the electronics and detector must be closely coupled. This is particularly true for use of an ionization calorimeter at the SSC because of the small signals and the necessity of extracting the maximum amount of timing information possible. In the following sections, we outline first the detector characteristics and the basic signal characteristics and amplification. The desired pulse shaping, and the extent to which it depends on the detector capacitance and properties of the cables, is discussed. The explicit dependence of the equivalent noise charge (ENC) and equivalent noise energy (ENE) on the detector and amplifier parameters is then presented. This is followed by a detailed discussion of the absorber and sampling pad configuration, the resulting detector capacitance, and the optimal cable parameters. Estimates of the risetime and electronic noise are then presented.

Other sources of noise include spontaneous disintegrations in the uranium plates and event pileup. The magnitude of the noise from these sources is evaluated and (from the total noise and the approximate shaping time) the time resolution is estimated.

Other important elements of the calorimeter electronics include the technique used for an analog pipeline, the required dynamic range, and the design of the Level 1 trigger; these are each discussed briefly.

Detector Characteristics

We shall assume in our consideration of the electronics performance and design that the primary calorimeter system utilizes liquid argon sampling with uranium or lead plates. The electromagnetic calorimeter is assumed to have a segmentation of $\Delta\eta \times \Delta\phi \approx 0.02 \times 0.02 - 0.03 \times 0.03$ with three longitudinal readouts; the hadronic calorimeter is assumed to have a transverse segmentation of 0.06×0.06 with a single longitudinal readout. These choices of segmentation, though not optimized, are believed to be reasonable estimates (supported by Monte Carlo calculations) of what is required if one is to adequately realize the physics goals that have been put forth.[14]

Liquid argon is *currently* one of the leading candidates for the sampling medium since it readily supports very fine segmentation, provides uniform response as a function of time and position, and can survive the intense radiation. Whether it will continue to be the sampling medium of choice in the future is less clear, and one might argue that the considerable uncertainty as to the type of calorimeter that will ultimately be employed renders detailed studies of the electronics somewhat premature. In fact, however, there appears to be relatively little uncertainty in the type of electronics that will be necessary. This is so because the size and segmentation of the calorimeter are reasonably well understood, and because nearly all ionization calorimeters, whether they employ liquid argon, silicon. a warm liquid such as TMP or TMS, or gas (at a relatively low gas gain) as a sampling medium, yield a signal of approximately 10 - 30 thousand electrons per minimum ionizing track and per sampling layer. While the drift time of the primary electrons may vary from 15 - 200 nsec depending on the sampling medium, the actual response time is dictated to a large extent by the charge collection time, i.e. the time required to transfer the charge from the detector to the feedback capacitor in the preamplifier.

Signal Characteristics, Pulse Shaping, and Noise

Signal Characteristics and Pulse Shaping Assuming a preamplifier with zero input impedance, and ignoring the capacitance and inductance of any connections, the current induced on a readout pad by a uniform ionization distribution throughout the liquid argon gap would be as shown in Figure 3. The maximum drift time t_d is approximately 400 nsec for a 2 mm gap if pure argon is utilized and 200 nsec for argon doped with 0.5% methane. In fact, the characteristics of the connections and preamplifier cannot be neglected and when taken together with the detector source capacitance, they can limit very significantly the charge collection time, independent of the actual drift time of the primary ionization.

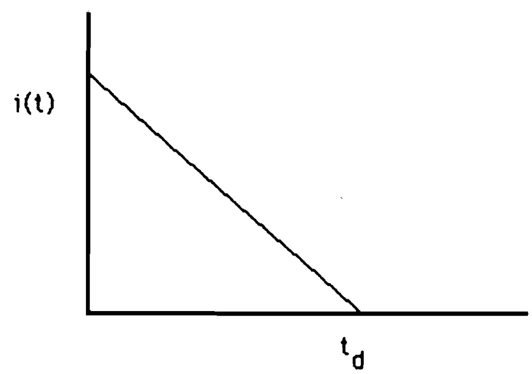

Figure 3
Current induced on a readout by uniform ionization distributed throughout a liquid argon gap.

A schematic diagram of the electronics is shown in Figure 4. For large detector capacitance (for example, $C_D > 1 - 10nF$) it is desirable to use transformers to match the amplifier input capacitance to that of the detector in order to maximize the signal-to-noise. It is essential that the properties of the connections, transformer, and preamplifier be chosen carefully to yield the minimal rise time without excessive ringing. A careful analysis[15] indicates that the minimum risetime that may be reasonably obtained is

$$t_r = 3.6T_d(1 + C_D/C_{cable})^{0.5}$$

where T_d is the total propagation time in the cable, C_D is the detector capacitance for that channel, and C_{cable} is the cable capacitance. Choosing $C_{cable} \approx 0.5C_D$ as a compromise between fast risetime and low noise yields $t_r \approx 40$ nsec $\times l$, where l is the length of the cable in meters between the readout pad and the preamplifier. Thus it is desirable to place the preamplifiers as close to the detector as possible, perhaps even placing them inside the liquid argon as is being done for the NA34 experiment. This option is not available, however, if the calorimeter is placed in a strong magnetic field and it is desired to use transformer matching. In this event, it may be necessary to locate the preamplifiers outside the magnetic field, which may require a cable length of 5 - 6 m.

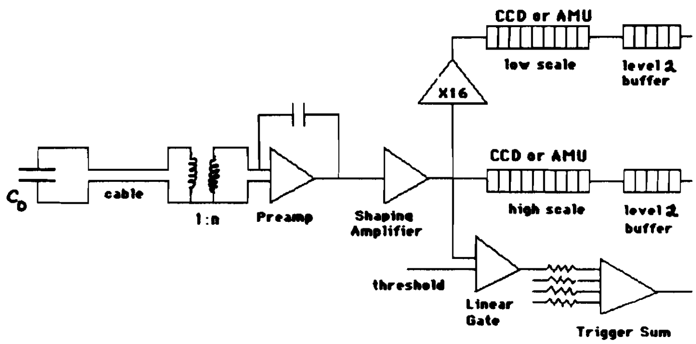

Figure 4
Schematic diagram of the front end electronics for the calorimeter. The output of the shaping amplifier is sampled and stored at 30 or 60 MHz in a CCD or analog memory unit (AMU).

There may also exist other reasons why relatively long distances between the detector and preamplifiers may be required. For example, if the preamplifiers are to be located inside the calorimeter it is essential that they be adequately protected against high voltage breakdown. In the absence of an adequate protection system, one may choose to locate the preamplifiers outside the cryostat for reasons of reliability. For the electromagnetic calorimeter towers, with a source capacitance of order 1.5 nF, one can dispense with transformer coupling without a large increase in the noise, and the preamplfiers could be located just outside the cryostat. In this event, a cable length of only 1-2 m might be obtainable. However, for our calorimeter design this would require bringing 175,000 signals through cold feedthroughs; this solution results in a very large heat loss and perhaps also in a reduced reliability of the cryogenic system.

The rather slow response produced by the inherent drift time in the liquid argon or by the slow risetime due to cables and preamplifier may be compensated to some extent by fast pulse shaping (with a corresponding decrease in the signal-to-noise). This is illustrated in Figures 5a-5c which show the performance measured for the NA34 system.[16] Figure 5a shows the response of the preamplifier to a δ function charge injection, (with the source capacitance attached), Figure 5b shows the response of the preamplifier to liquid argon signals and Figure 5c shows the response after bipolar shaping. The peak of the signal, which is proportional to the energy deposition, is attained after 100nsec. The time of the signal may also be determined rather accurately from the zero crossing point.

As a compromise between the requirements of fast response, particularly in the trigger, and the difficulty and/or expense of bringing in excess of 200,000 signals through the cryostat, it was proposed that both the hadronic and electromagnetic calorimeters have fast trigger signals corresponding to a segmentation of 0.06×0.06 with 1 longitudinal sum. The fast response would be attained by bringing the signals directly through the cold feedthroughs and minimizing the cable length as much as possible. For the hadronic calorimeter this is the shortest path length to a field free region, a distance of 5 - 6 m. For the electromagnetic calorimeter, the distance could be as short as 1 - 2 m if the preamplifiers were mounted directly on the outside of the cryostat. The electromagnetic calorimeter would in addition have slower readouts with the full 0.03×0.03 transverse segmentation and three longitudinal samples. The cables

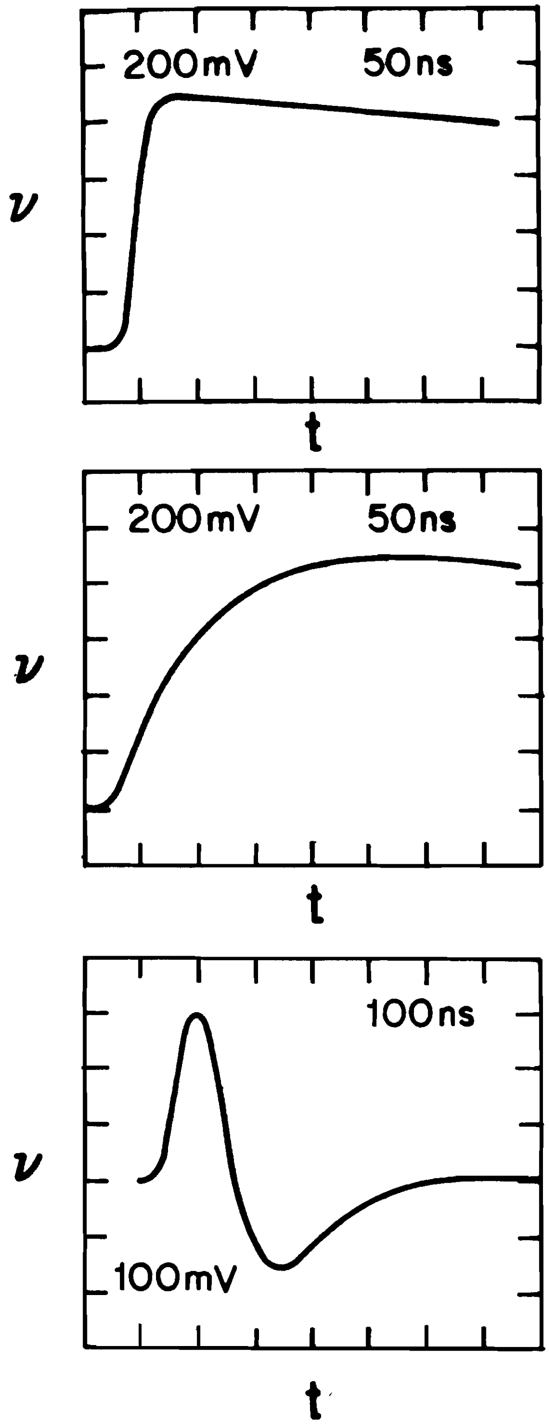

Figure 5
Measured response of the NA34 liquid argon calorimeter system. (a) Output of preamplifier for δ function charge input. (b) Output of preamplifier for liquid argon signal. (c) Output of fast shaping amplifier for liquid argon signal.

transporting these signals to the preamplifiers would exit the calorimeter through gas ports at the top, thereby resulting in cable lengths of approximately 12 m. The trigger signals would almost certainly be subjected to bipolar shaping to enable accurate time measurements. In the analysis below of (1) electronic noise, (2) equivalent noise due to pileup of events, and (3) time resolution, we have assumed utilization of bipolar shaping such as that illustrated in Figure 5 for all three types of readout.

Equivalent Noise Charge An approximate expression for the equivalent noise charge (ENC) arising from noise in the preamplifier is

$$ENC \approx 1.5 \times 10^3 (C_S)^{.5} (t_a/t_m)^{.5}$$

where we have assumed a reasonably low noise FET, optimal transformer matching ($n_{opt} = (C_S/C_A)^{.5}$), and unipolar shaping. The total source capacitance is denoted by C_S and the amplifier input capacitance by C_A. The time delay between particle incidence and the peaking of the signal, which we will refer to as the measurement time, is denoted by t_m; t_a denotes the characteristic time constant of the FET and is typically of order 0.5 - 1 nsec. In the event that transformer matching is not utilized, or the matching is deliberately mismatched (for example to improve the damping), the noise increases according to

$$\sigma/\sigma_{opt} = 0.5(n_{opt}/n + n/n_{opt}).$$

For bipolar shaping, the noise increases by $\sqrt{2}$; in addition, in the calculations below we will also increase the estimated noise by 1.2 to allow for the additional effects in a real system. The resulting expression then agrees reasonably well with measurements (for example for the Helios calorimeter of NA34).

Equivalent Noise Energy To equate the noise in electrons to an equivalent noise energy, one must determine the mean number of ionization electrons collected per Gev of energy. We shall use the expression

$$\#electrons/GeV = 10^9 S/24.6eV \times 0.5$$

where S is the sampling fraction

$$S = (dE)_{LA}/((dE)_{LA} + (dE)_U + (dE)_{G10})$$

$$dE/dx_{LA} = 2.2MeV/cm$$

$$dE/dx_U = 22MeV/cm$$

$$dE/dx_{G10} = 3MeV/cm$$

and it requires on average 24.6 eV energy loss to produce an electron ion pair in the liquid argon. The factor 0.5 arises from the empirical observation that the charge produced per GeV is approximately one-half as large for electrons and hadrons as for muons.

The above represents the charge *produced* per GeV in the liquid argon. To obtain the effective charge detected per GeV, one must in addition multiply by 0.5 to allow for the fact that the induced charge on the pad is 1/2 that produced, and by the *ballistic deficit* a. The coefficient a is near 1 if the drift time of the electrons, and the rise time of the preamplifier are both small compared with the shaping time constant τ. Neither of these conditions is true in general for our application, and a will typically take on values between 0.3 and 0.6

Calorimeter Sampling For the purpose of estimating the above quantities, we assume that the longitudinal sampling of the electromagnetic calorimeter is constructed of 40 cells, where each cell consists of a 2 mm uranium plate, 2mm LA gap, 1.6 mm G10 printed circuit board, and an additional 2 mm LA gap. The transverse size of the pads is taken to be $5cm \times 5cm$. The hadronic cell is assumed to be identical except that the Uranium plate is 6 mm thick and the transverse size of the pads $20cm \times 20cm$.

The fast trigger signals for the electromagnetic towers are obtained by summing 2×2 arrays of pads transversely and by summing the ouputs from alternate cells longitudinally; the intervening cells then provide the slower, more finely segmented readout signals. An alternate possibility, which clearly has some advantages in terms of minimizing sampling fluctuations, is to use the signal from one LA layer in each cell for the fast readout, and the signal from the other LA layer for the slow signal. However, in that case it would probably be necessary to isolate the pads on the two sides of the G10 board with a ground plane; this would greatly increase the capacitance, and it was therefore decided to sum alterate cells.

Detector Capacitance To accurately determine the total source capacitance one must include the capacitance from the cables and from the strip lines on the G10 boards. Each of these can be quite large and in fact dominate in some instances.

The additional capacitance due to the readout strips depends in large measure on whether it is necessary to shield the readout strips and the pads with ground plane in order to minmize the crosstalk. The crosstalk depends on the length of the readout traces which in turn depends on the size of the readout board. We shall assume for the electromagnetic calorimeter G10 boards which are $40cm \times 40cm$ and which therefore contain 64 pads per board. Since the printed circuit board or cable which sums the layers longitudinally necessitates a crack of several millimeters, with a corresponding nonuniformity of response, use of smaller boards is detrimental to the overall uniformity of the calorimeter. Larger boards may be feasible but increase further the stripline capacitance and may also increase the cost. If the signals are transported to one side of the board for summing, then the number of traces beneath each pad will vary between zero and seven depending on whether the pad is far or near to the summing edge. Assuming a triangular ground plane which is just sufficient to overlap the traces, we estimate that the additional capacitance between the strips and the ground shield, and the ground shield and the pads, is of order 40 pF per pad. The basic detector capacitance between the pads and the absorber plates is 35 pF per pad. Thus the total detector capacitance per finely segmented tower is $C_D \approx$ 7 layers * 75 = 525 pF.

The fast EM readout sums 2×2 arrays of pads and the number of readout traces is correspondingly fewer. We estimate the stripline contribution to the capacitance as 40 pF and the basic capacitance for each layer as 140 pF. Then the total capacitance for the fast EM towers is $C_D \approx$ 20 layers * (140 pF+ 40 pF) = 3.6 nF.

Finally we note that for the hadronic towers, which are $20cm \times 20cm$, the number of strips traversing each pad is either 0 or 1. In addition, crosstalk between adjacent towers of a fraction of a per cent is likely to be negligible compared to the inherent width of the hadron shower. Use of the additional ground plane to shield the traces should be unnecessary and any capacitance due to the striplines will be negligible compared to the basic detector capacitance of 51 nF.

Cable Capacitance The cables will be tailored to yield the optimal risetime and signal-to-noise for each type of tower. Using the expression for the risetime

$$t_r \approx 3.6 T_d (1 + C_D/C_{cable})^{0.5}$$

a reasonable compromise between risetime and signal-to-noise is obtained by $C_{cable} \approx 0.5 C_D$. For the slow EM readouts this would imply $C_{cable} \approx 260$ pF; however, given that these cables are 12 m long this would imply a capacitance per meter of 22pF which is difficult to obtain. We assume 75pF/m which corresponds to $Z \approx 80\Omega$ (if the propagation delay is 6-7 nsec per m). Thus the total source capacitance is $C_s \approx 525 + 900pF = 1.4nF$ and $t_r \approx 325$ nsec.

The fast EM towers have $C_D = 3.6$ nF thus implying $C_{cable} \approx 1.8$ nF. Since these cables are only 1.5 m long, we assume 1.2 nF/m which correponds to $Z \approx 5 - 6\Omega$. Then $t_r \approx 65$ nsec.

Finally for the hadronic calorimeter towers, the above guideline would suggest $C_{cable} \approx 26$ nF which corresponds to an unreasonably large value for 6 m of cable. We assume 1.5 nF/m which implies $C_s = 51 + 9 = 60$ nF and $t_r \approx 365$ nsec.

The source capacitance for each type of readout is summarized in Table 1. This information is combined with an assumed measurement time, shaping function, and resulting ballistic deficit to also yield the ENC and equivalent noise energy.

Table 1 Summary of Capacitance, Equivalent Noise Charge, Equivalent Noise Energy, Risetime, Event Pileup, and Time Resolution for the Calorimeter System

Quantity	Symbol	EM Slow	EM Fast	Hadronic
Pad Capacitance	C_{pad}	0.25 nF	2.8 nF	51 nF
Stripline Capacitance	C_{strip}	0.28 nF	0.8 nF	
Cable Capacitance	C_{cable}	0.90 nF	1.8 nF	9 nF
Total Capacitance	C_{source}	1.4 nF	5.4 nF	60 nF
Risetime	t_r	325 nsec	65 nsec	365 nsec
Measurement or Peaking time	t_m	400 nsec	100 nsec	500 nsec
Equivalent Noise Charge	ENC	4800 e	25000 e	30000 e
Equivalent Noise Energy	ENE	15 MeV	65 MeV	120 MeV
Uranium Noise Energy	σ_{ur}	5 MeV	7 MeV	170 MeV
Event Pileup Noise		115 MeV	120 MeV	113 MeV
Time Resolution (E = 5 GeV)		4 nsec	2 nsec	8 nsec

Uranium Noise

To estimate the noise due to the natural radioactivity of the uranium we have scaled according to a formula used by D0:

$$\sigma_u(MeV) \approx (0.12/S)\sqrt{A\tau}$$

where S is the sampling fraction, A is the pad area in square meters, and τ is the effective sampling time in nanoseconds. The results obtained for each tower type are presented in Table 1.

Equivalent Noise from Event Pileup

The effective noise due to event pileup is potentially one of the greatest uncertainties in the measurements of energy and considerable effort was therefore devoted to studying this effect. Two groups performed similar but independent calculations: in each case a mixture of minimum bias and jet events were generated using ISAJET and the particle energies deposited in a hypothetical calorimeter with an appropriate segmentation and distance from the vertex. For each study sinusoidal bipolar shaping was assumed and the observed energy in a given tower at a given time was the sum of the contributions from all crossings weighted appropriately by the shaping.

Yamashita and Kondo[17] assumed an electromagnetic calorimeter with a rapidity-ϕ segmentation of 0.03×0.03 and two longitudinal readouts; the hadronic segmentation was 0.06×0.06 with one longitudinal readout for the "precision" calorimeter and one for the "tailcatcher". The energy deposited in a given tower could arise from particles hitting any of the adjacent towers as well as from particles hitting that tower directly. The sharing of energy between different sections of the calorimeter was determined using average transverse and longitudinal shower profiles. Fluctuations in the width and length of showers were included and the initial interaction point for hadrons was generated according to the expected exponential distribution. Prior to interaction, hadrons deposited energy according to the average ionization loss expected for a minimum ionizing particle. Figures 6 and 7 show the RMS energy in the first section of the electromagnetic calorimeter (9 radiation lengths) and in the precision section of the hadronic calorimeter (6.2 interaction lengths) as a function of rapidity and shaping time.

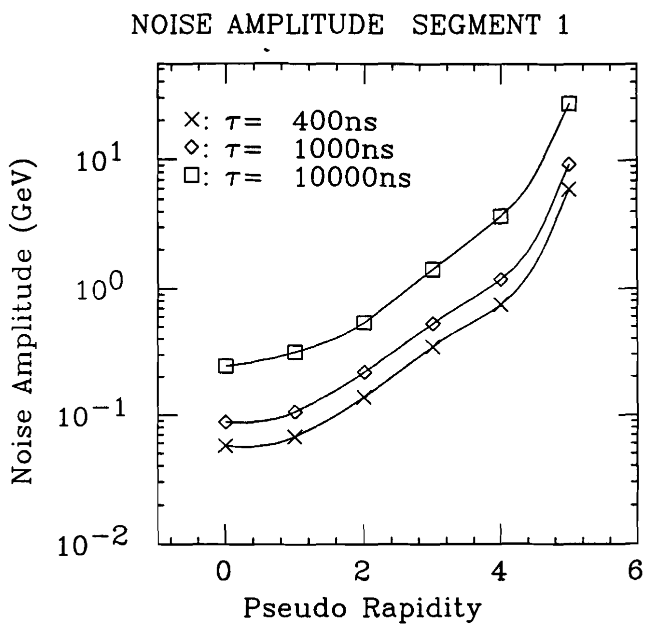

Figure 6

Equivalent RMS energy "noise" in the first section of the electromagnetic calorimeter (9 radiation lengths) due to event pileup as a function of rapidity and shaping time.

Alverson and Huston[18] performed a similar calculation, though without attempting to share the energy among the towers. They assumed a segmentation of 0.06×0.06 and verified explicitly that the noise scales as the square root of the shaping time and the area.

Comparison of the two calculations for the electromagnetic calorimeter is rendered somewhat uncertain since one does not know exactly how to combine the rms noise for the two EM longitudinal sections. If we assume they are uncorrelated (an underestimate), we obtain from Yamashita and Kondo's calcu-

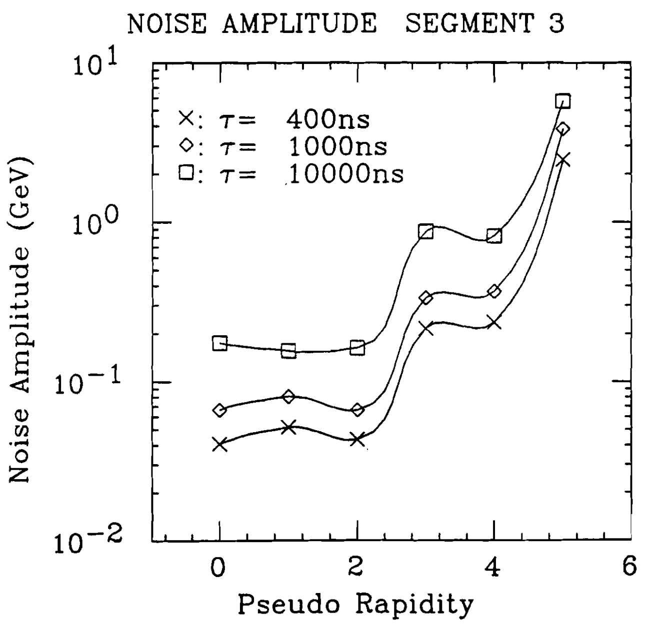

Figure 7
Equivalent RMS energy "noise" in the precision section of the hadronic calorimeter (6.2 interaction lengths) due to event pileup as a function of rapidity and shaping time.

lation $\sigma \approx 100 MeV$ for 0.03×0.03 and $\tau = 1000$ nsec. Alverson and Huston estimate 70 MeV. For the hadronic calorimeter, the comparison is more straightforward. For $\Delta\eta \times \Delta\phi$ 0.06×0.06 and $\tau = 1000$ nsec, the former calculation yields ≈ 80 MeV and the latter ≈ 330 MeV. The rather large discrepancy presumably arises because of the rather large difference in how the energy of hadrons is deposited. We note that it is observed by UA1 and UA2 that for a minimum bias trigger nearly 80% of the event energy is deposited in the EM calorimeter. We conclude that the energy sharing is therefore important in estimating the noise due to pileup. Table 1 gives the noise due to event pileup for each of the three hypothesized readout configurations.

Energy Measurement and Analog Pipeline

Following the shaping amplifier (which may produce either unipolar or bipolar signals), the front-end electronics system must perform at least the following functions:

1. energy measurement, via sampling of the voltage at the appropriate time
2. time measurement for at least the trigger towers
3. storage or delay of the analog information until the Level 1 trigger is completed (≈ 0.5 usec)
4. buffering of the information from events that have passed the Level 1 trigger so that additional events may be recorded in a deadtimeless way.

These goals may be accomplished in a number of ways. For example, in one of the simplest schemes the delay could be provided by a conventional delay line and the energy determined by two sequential samplings, one before the event of interest and one after the event of interest. The time of the sampling would be generated by the trigger with careful attention paid to the propagation delay through the system; each Level 1 trigger, whether it corresponded to the Level 1 requirement for a muon, electron, high p_t jet, or large missing E_t would generate a trigger at the correct time so that the energy in the calorimeter would be correctly measured for the event producing the trigger.

It is generally accepted that in a high rate environment unipolar shaping with two samples is not sufficient; it is necessary to measure the slope of the baseline as well as its magnitude. This is then equivalent to "bipolar shaping". In addition, it will be essential to measure the time of energy depositions in at least the trigger towers. Because bipolar shaping is the natural choice for time measurement (the zero-crossing time is independent of the amplitude) and because the zero-crossing time may be easily and accurately measured by additonal voltage samples, the system which shown in Figure 4 seems a natural choice. The desirability of a front end system that is deadtimeless (or nearly so) suggests an analog pipeline, or "analog ring buffer", that accomplishes all of the other objectives and eliminates the need for a delay line. Produced in large quantities, it is probably cheaper than delay lines.

The actual technology and design that will be utilized to implement the analog pipline is not completely clear at this time. It can probably be accomplished with appropriate CCD's or with a multiplexed capacitor array such as the *Microstore* recently designed for use with SLD.[19]

Dynamic Range

The dynamic range of the system is set by the maximum energy that must be measured without saturation and by the precision that is required at low energies. The most stringent criteria at the upper end of the scale is probably set by the search for Z bosons with masses in the range of 4 - 6 TeV; this implies that one must be able to measure energies of order 2 TeV in a single channel. At the low end, the inherent resolution of 12 - $15\%\sqrt{E}$ for the electromagnetic calorimeter implies a resolution of 120 - 150 MeV at 1 GeV. One does not want to compromise this resolution since it is likely to be important for the determination of the position of electron showers. A scale of 100 MeV per ADC count is consistent with this; at the same time the inherent limitations due to electronic noise, uranium noise, and event pileup will probably prevent any substantial benefit from a finer scale. Hence, the dynamic range of the system must be of order 14 bits.

Current systems, such as that for the CDF calorimetry, have demonstrated the feasibility of obtaining dynamic ranges equivalent to 16 bits in a relatively straight-forward and inexpensive way.[20] While the preamplifier incorporates the full dynamic range, it is often simpler and less expensive to divide the signal at some point such that two parallel, overlapping systems of lesser dynamic range are utilized to accomplish the overall objective. Since both CCD's and multiplexed capacitor systems are currently rather far from 14 bit performance, we assume two parallel systems, each of 9-10 bit accuracy, as shown in Fig 4.

Triggering

The calorimeter information will be extremely important for triggering and will be used to select events with electrons, high p_t jets, large total transverse energy E_t, and large missing momentum. The fast bipolar shaping discussed above is probably the optimal signal processing for an application in which both energy and time resolution is important, as is the case here. We now discuss briefly how this information may be used to form initial triggers.

It has been found useful, both in offline analyses and particularly in the formation of triggers, to exclude from energy sums those towers whose energy is below a certain minimum, E_{towmin}. This will be particularly true in the present high rate environment due to the significant amount of low energy noise, which arises both from pileup and from electronic noise. A schematic diagram of a simple analog switch, which passes the information linearly if it exceeds a certain threshold, is shown in Figure 8. We anticipate that such a switch will be utilized for each 0.06 × 0.06 trigger tower, though it is conceivable that direct analog sums of 2 - 4 towers might be performed first if coarser segmentation proves to be adequate.

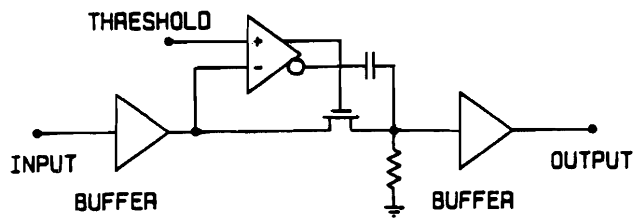

Figure 8
A schematic diagram of a simple analog switch which passes the information linearly if it exceeds a certain threshold.

In performing larger sums of towers, e.g. to obtain jet energies, total transverse energies, or total missing E_t, it is important to sum only those energies which can be associated with a particular beam crossing. It has already been shown in Table 1 that the time resolution should be sufficient to uniquely identify an energy deposition with a given crossing, if the energy is in fact sufficiently large to be relevant to the trigger. The inclusion in a sum of only those tower energies identified with a given time or beam crossing could be implemented in a variety of ways, using either analog or digital techniques. As an example of the former, the output of the sample-and-hold circuit which samples the energy at time t_m could be gated with a narrow-width pulse at the time determined by the zero-crossing point; the output would then be a pulse of 5 - 10 nsec width, the amplitude of which would be proportional to the energy. Direct analog sums could then be formed which included only those energies associated with each crossing. One would have the option of including or excluding energies for which the zero-crossing time did not correlate with a particular interaction, thereby indicating sustantial contributions from more than one event. More detailed studies are clearly required to indicate the optimal strategy.

Alternatively, the energy sampled at time t_m could be immediately digitized, and the zero crossing time would determine whether that information is included in the sum corresponding to a particular beam crossing.

In all likelihood, a combination of both analog and digital techniques may be utilized. Digital sums have the advantage of minimizing settling times, particularly for sums which combine information from widely separated parts of the detector, while analog techniqes are probably simpler and more efficient for sums over a local region.

TRACKING ELECTRONICS

Introduction

It is well known that the environment created for particle tracking by the high multiplicity and event rate at a machine such as the SSC is very severe. Potential problems include event pileup, distortion of the gain and drift velocity due to the equilibrium level of ions, and radiation damage. In addition, the segmentation required in order to achieve reliable and efficient pattern recognition is very large. Studies of the Tracking Group[3] at this workshop, and also in the 1984 Snowmass summer study,[21] concluded that adequate tracking can be achieved *provided* that one utilizes low gas gain, fast pulse shaping, and cell sizes of 3-10 mm diameter, with a correspondingly large number of wires (of order 10^5 for the central tracking alone). While there are significant mechanical problems that must be addressed concerning how one supports this many wires without introducing an unacceptably large amount of material, to a large extent the problems of tracking become identified with the problem of developing an electronic system which *simultaneously* satisfies the requirements of low noise, low power, and high speed.

A major goal of the electronics group was (1) to determine the *feasibility* of an electronics system which satisfied the desired goals, (2) to outline a schematic diagram of such a system, and (3) to identify, at least to the extent possible at a workshop of this nature, the most important research and development required.

Tracking systems for SSC detectors will in fact consist of many different types of detectors and readout including in all likelihood central tracking, intermediate tracking, forward tracking, transition radiation detectors, and a microvertex detector. There are at least three different types of electronics systems that may be utilized, depending on the quantity which it is desired to measure. These include

1. Measurement of the total charge (or a fixed fraction of the total charge) deposited by individual particles.

2. Measurement of the time of the signal from individual particles.

3. Measurement of the charge, as a function of time, resulting from one or more particles (waveform sampling).

It may be desired to make these measurements either on the signals induced on the wires (anodes) or on the cathodes.

It is important to distinguish between the requirements of (1) in which only one charge is measured per particle, and the rate of measurement is set by the instantaneous rate of particles (typically 3 - 6 Mhz) and the beam crossing rate (60MHz), and (3) in which multiple measurements of charge from a single particle are made either to obtain good timing resolution or to separate the charge distributions from different particles with spacing as close as 20 ns. The latter system, which we will refer to as waveform sampling, typically requires sampling frequencies of at least 100 MHz and preferably 200MHz.

It is very likely that all three types of systems will be employed, with the relative numbers of channels depending on the final track chamber design which is far from optimized. Measurements of total charge will almost certainly be employed for silicon detectors, for pad readout of some of the wire chambers in order to determine the z coordinate, and for TRD's. The relative importance of (2) and (3) depends on the extent to which one attempts to use (a) small diameter cells of square, circular, or hexagonal geometry in which only a single particle per event is measured or (b) cells which have a sufficiently long drift time and a geometry such that multitrack detection is warranted. It is the conclusion of the Tracking Group that the very high particle flux and questions of radiation damage force a large part of the chamber, if not the total chamber, to utilize cells of type (a).

The electronics group decided to concentrate on systems of type (2) because a large fraction of the tracking electronics will be of this type and because it seems more likely that electronics of this type might be incorporated directly on, or very near to, the chamber itself. In addition, there already exists a broad development effort on low power, extremely compact systems of type (1) which are necessary for the readout of silicon detectors and cathode pads.

Specifications and Performance

If the electronics system is not to limit the performance of the tracking systems being proposed, it must satisfy the following goals:

1. Sufficiently low noise to allow operation with gas gain of order 1 - 2×10^4
2. Time resolution < 1 nsec.
3. Double pulse resolution of 20-30 nsec

The first criterion must be met if the chamber lifetime is to conservatively exceed several years. The second corresponds to an electronics contribution to the position resolution of 50 microns for a gas with conventional drift velocity of 50 microns/nsec and 100 microns for a "fast" gas with $v_d \approx 100$ microns/nsec. The third condition must be satisfied if the efficiency per wire is to exceed 90%. A schematic diagram of the system for measuring drift times is shown in Figure 9.

Fortunately, the continuing evolution and refinement of preamplifiers[22] and amplifiers has led to systems which are capable of the performance represented by (1) - (3). Of particular interest has been the development of rather simple, yet fast, shaping amplfiers capable of producing pulses of FWHM ≈ 6 nsec. Figures 10a - 10c illustrates the performance of one such system which utilizes delay-line clipping to suppress the exponential tail of the preamplifier and pole-zero cancellation to nearly eliminate the 1/t falloff of the current pulse from the chamber. A four-fold integration with time constant ≈ 1 nsec is utilized as an approximation to gaussian shaping. These results were obtained with a very small chamber, but even for relatively large chambers it should be possible to obtain pulses with FWHM $\approx$ 12 - 15 nsec. It therefore seems feasible to achieve an electronics double pulse resolution of < 30 nsec.

Given the shaping discussed above, the effective time resolution such that two independent tracks can be resolved will be determined primarily by the time during which the ionization from a single particle is collected. For a cell with an aspect ratio of 1:1 the charge collection time is of order the maximum drift time. For cells of maximum drift distance ≈ 1 mm, which may be utilized in the central tracking at small radii (of order 30 - 50 cm) and in the forward direction, the total collection time, assuming a gas with conventional drift velocity 50 microns/ns, is less than 20 nsec. However, a very large number of cells in the central region will likely have a maximum drift distance of order 2 - 3 mm. For these cells a faster gas, with $v_d \approx$ 100 microns/nsec would be a great advantage. CF_4 has been utilized at these drift velocities[23], but its suitability in terms of radiation damage has not been proven. A systematic search for faster gases which are radiation hard and suitable in other regards is clearly very important.

Power

A fourth very important goal, not mentioned above, is that the entire system- preamplifier, amplifier, discriminator, and time measurement- should consume less than 100mW of power. Obtaining the performance discussed above with such a low power is a non-trivial challenge; typical current systems consume of order 0.5 - 1 watt per channel.

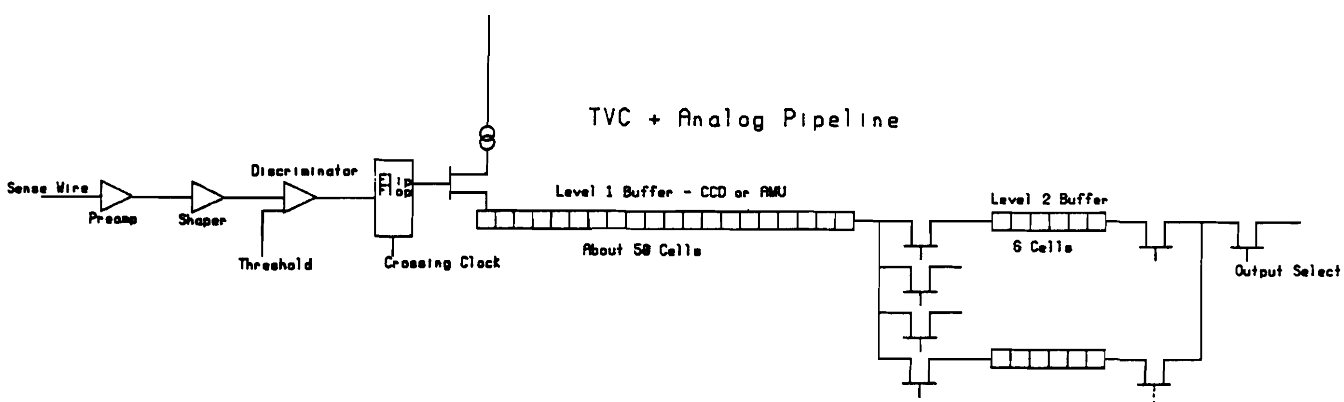

Figure 9
Conceptual design of the electronics for measuring drift times in a track chamber. In addition to a preamplifier, shaping amplifier, and discriminator, the circuit schematically shows time-to-voltage conversion followed by an analog buffer.

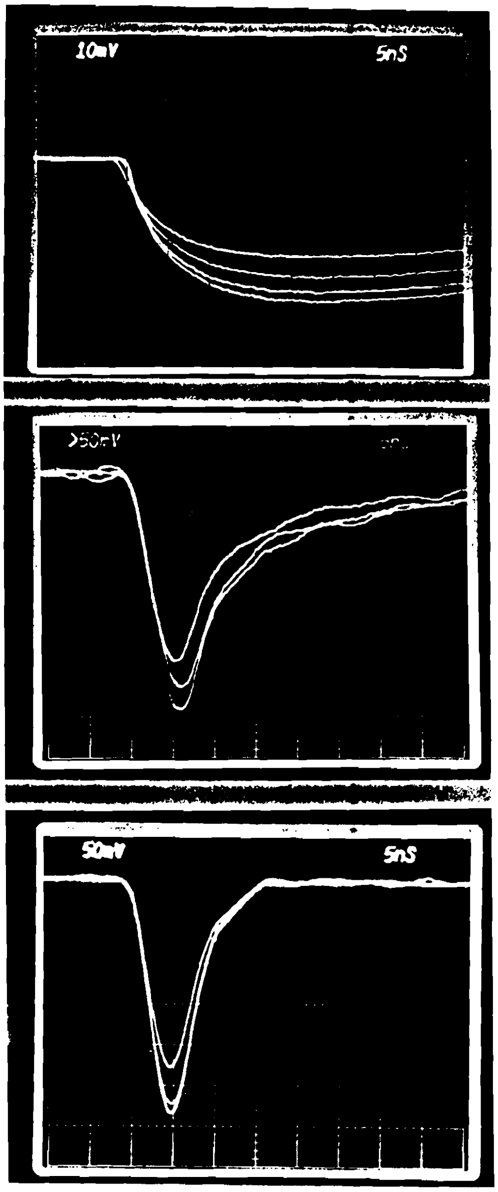

Figure 10
Performance of a fast shaping amplifier with delay-line clipping. (a) preamplifier output, (b) preamplifier tail cancelled (which is approximately the anode current) and (c) the signal with the current tail cancelled.

The motivation for such a low power is partially economic since the cost of crates, cooling, power supplies, etc. is to a large extent proportional to the total power. But the strongest motivation is provided by the desire to locate the entire front-end electronics system, up through the time measurement and digital or analog pipeline, directly on, or very near to, the chamber endplate. The alternative, which is routing 50,000 to 100.000 cables to electronics at a remote location (even if remote is only 5 m distance), appears to be extremely difficult to accomplish without seriously degrading the hermeticity of the calorimetry. While a clever mechanical design may produce a technique for integrating so many cables with the calorimetry in an innocuous way, the preferred solution seemed clearly to be location of the entire system near the chamber. In this way only those signals required for a trigger, and a small number of cables that are used for the multiplexed readout, need be brought out. While access to the electronics would be limited, it was felt that careful consideration of system design and redundancy would yield a system that was sufficiently reliable.

Time Measurement

Two different systems were considered for time measurement. The first, schematically illustrated in Fig. 9, uses time-to voltage conversion and an analog pipeline. A pulse from a wire, which exceeds the discriminator threshold, turns on a current source, which is then turned off by the subsequent pulse from a reference clock system. It is presumed that the reference clock would be synchronized to the beam crossings and would run at 0.5 or 1 times the crossing frequency, that is 30 or 60 MHz. The goal would be to obtain a time resolution, at least in the absence of slewing or "walk" effects, of 200 - 300 picoseconds and a full scale range of $\approx$ 15 - 30 nsec. Numerous such systems have been built using discrete components and there is no fundamental reason why such performance could not be obtained with fully integrated, or largely integrated, systems. The required dynamic range of the analog memory or analog pipeline would then be $\approx$ 8-9 bits. It seems likely that either CCD's or switched capacitor arrays could be utilized, though research and development is clearly required.

A purely digital system (Figure 11) for the time measurement was also proposed[24]. The basic idea is that a narrow

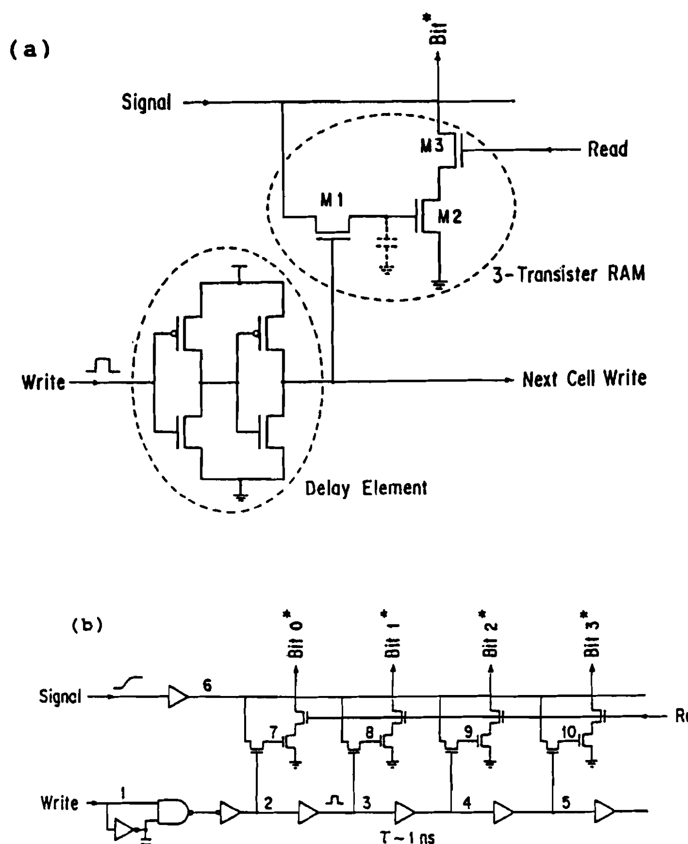

Figure 11
(a) Basic Time Memory Cell. Charge is stored in the gate capacitance of M2 Transistor. (b) Row Memory Cells. Numbers indicated are node numbers.

pulse, approximately 2 nsec in width and synchronized with the crossing time, passes through a series of gates each of propagation delay 1 nsec. The output of each gate is the Write Enable for a three gate memory cell. The signal from a given wire, appears simultaneously at the Data Input for each memory cell; those cells at which the write pulse appears prior to a signal will register 0, while those cells at which the write pulse appears after the signal will register 1. Some preliminary simulation of the circuit and study of variations in the propagation time due to changes in temperature and supply voltage indicate that an accuracy of 1 nsec is obtainable. Assuming that the crossing time is 16 nsec, it is suggested that the device be configured in rows of 16 memory cells. If the maximum drift time in the chamber is 100 nsec, 6 rows would be sufficient to contain all information for a given event. A total of 32 rows would provide the 500 nsec memory time required for the Level 1 trigger.

Buffering and Readout

Whether a digital or analog system is utilized for the time measurement, the buffering and readout is presumed to occur in the same fashion. The analog or digital pipeline is sufficiently deep to store data for approximately 32 -64 crossings (500 - 1000 nsec). Upon receipt of a Level 1 trigger, the data from the event of interest is transferred to a Level 2 buffer. It is imagined that there might be four such buffers and that it is possible to write to the buffer in less than 16 nsec; the system is then deadtimeless. If the analog pipeline is implemented with switched capacitor techniques, then the Level 2 buffering may be implemented without actually transferring any data; one simply removes the storage elements corresponding to the event of interest from the "active" list of elements being utilized for the initial analog pipeline.

Should one of the events passing the Level 1 trigger also pass the Level 2 trigger, then readout of the information would commence. It is generally presumed that the combined Level 1-Level 2 trigger system reduces the rate by 10^5 to ≈ 1 kHz. Assuming 100k wires, and an occupancy of 10%, implies 10k channels to be readout. We conservatively assume a readout time per hit of 1 μsec, and conclude that 100 cables (and 100 ADC + Scanner systems) would be sufficient to complete the readout in ≈ 100 μsec.

Waveform Sampling

Waveform sampling in its idealized form is the most powerful electronics technique for tracking electronics in that all the information content of the original signal is preserved. Time information is preserved for leading edge timing with walk corrections or for center-of-gravity timing for diffusion limited cases, as well as for delay line techniques. Charge information exists for energy loss determination and for charge division measurements. In addition, all this information exists for multiple tracks from the same or overlapped interactions. However, the large information content implies substantial power consumption for data storage and buffering and implies a significant data acquisition and processing burden to extract the desired quantities. In principle, any subsequent processing of digital waveform samples can be accomplished (in an inflexible fashion) by analog circuitry between preamplification and sampling. The choice of whether or not to employ waveform sampling will depend on the particular tracking element and on the flexibility needed in extracting measurements. Several techniques for waveform sampling, such as Flash ADC's, CCD's, and switched capacitor arrays (analog memories), now exist, offering a range of sampling speeds and dynamic ranges.

TRIGGERING: LEVEL 1 AND LEVEL 2

Triggering for experiments at SSC was discussed in some detail at the Triggering, Data Acquisition, and Computing Workshop held at Fermilab in November 1985. In the following we draw freely on some of the conclusions and ideas of that workshop. New contributions focused on particular aspects of Level 1 triggers.

The Level 1 trigger, because it must complete its task in ≈ 500 nsec, will primarily be formed from relatively simple sums and comparisons (both analog and digital) of data from a subset of the detectors. However, there will be some exceptions to this, such as for the forward muon system (discussed below) where momentum determination by means of a fast, analog, least-squares-fit will be required at Level 1.

Level 2, with 10 - 30 microseconds available, will make extensive use of special hardware processors (primarily digital) to refine Level 1 triggers, to perform operations which cannot be executed in Level 1 due to the time constraints, and to correlate the data from different types of detectors with greater generality than can be done at Level 1.

Level 1 Triggers

One of the important assumptions in the trigger systems that have been proposed is that one can obtain a rejection factor $10^3 - 10^4$ within 0.5 - 1 usec. That is, the rate of "interesting" events that pass the Level 1 system should be reduced to $10^4 - 10^5$ per second, since it is presumed that Level 2 triggers will require of order 10 - 30 μsec.[25] The strategy of Level 1 is to identify "candidates" for particular types of particles, such as electrons, muons, quarks, etc., in a manner that has high efficiency but is still moderately selective. The Level 1 triggers that are typically regarded as crucial for selecting the events of interest are

1. Total E_t and missing p_t
2. Jets with $E_t > 40$ GeV
3. Isolated electrons with $E_t > 25$ GeV
4. Muons with $p_t > 10$ - 15 GeV

A fifth category which is more often listed among the Level 2 triggers, but which is a candidate to be included in Level 1, is that of high p_t tracks.

Trigger Times and Pipelining As indicated by the calculations on time resolution for the calorimeter, it should be possible to uniquely associate an energy deposition in a particular trigger tower with a particular beam crossing, if the energy deposition is sufficiently large to be important for the Level 1 trigger. Since it is necessary in any event to have a one-to-one correspondance between a particular trigger and the raw data corresponding to that trigger, and since it may be useful even at Level 1 to combine trigger information from different detectors, it is presumed that the output of any trigger system, e.g.

electron, muon, jet, missing E_t, etc., will have a time associated with it which allows that trigger to be uniquely identified with a particular crossing. If analog memory units or shift registers are used to pipeline the trigger information in the same manner as for the raw data, it is then straightforward to form combinations of triggers in a manner that is deadtimeless.

Calorimeter Triggers The calorimeter information will be extremely important for triggering and will be used to implement categories (1) - (3) above.

A brief description of some of the techniques that might be used in forming fast sums for the calorimeter tirggers has already been presented. Here we note that these triggers also require that one be able to multiply the energy in each tower, or the energy sum of several towers, by $\sin\theta$, in order to calculate the transverse energy E_t, and by $\sin\phi$ or $\cos\phi$ in order to calculate the vector missing E_t. Given the pipelined structure, it should be possible to accomplish this either with multiplying DAC's or with digital multipliers, and still be able to keep the association of each trigger with a particular crossing.

The jet trigger will require some form of crude clustering at Level 1. Both the UA1 and UA2 experiments found it important to include this capability so that prototype systems exist.[26] While there has not been any detailed consideration of how to best implement it at the SSC, a straightforward procedure, which may be adequate, is that of summing all those trigger towers within a region of order $\Delta\eta \times \Delta\phi \approx 1 \times 1$; in order to maintain efficiency such sums would have to be overlapping. It is also quite likely that more sophisticated clustering techniques will be developed that are sufficiently fast.[27-29]

Electron Trigger The basic electron trigger consists of the requirement that there exists a cluster of energy, E_{em}, in the electromagnetic calorimeter which exceeds a certain minimum threshold, for example 25 GeV, and which is largely electromagnetic; the latter criterion is implemented by requiring the hadronic energy, E_{had}, directly behind the electromagnetic cluster to be less than a certain fraction of E_{em}, for example $E_{had} < 0.1E_{em}$. The clustering in its simplest form may simply be the sum of the energy in four trigger towers. In order to obtain full efficiency, one must allow for energy sharing between trigger towers; hence each four-tower sum will presumably be offset from the adjacent sums by one trigger tower width (0.06) in rapidity or azimuth. This is the scheme used very effectively by the UA2 experiment. A schematic diagram, put forth at the Fermilab workshop, of how the trigger could be accomplished is shown in Figure 12.

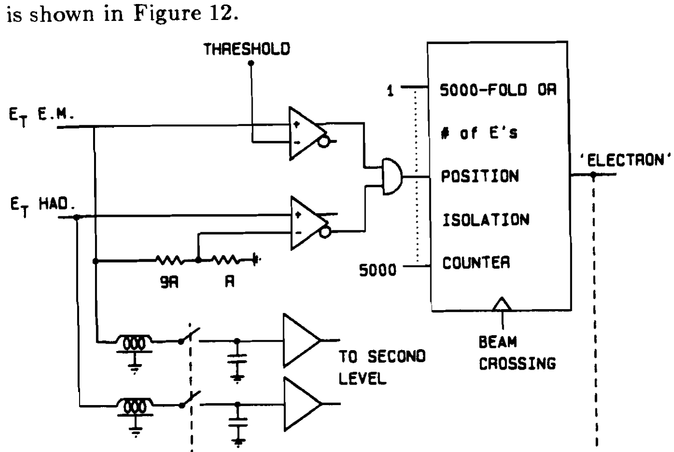

Figure 12
A schematic diagram of the electron trigger logic.

A further refinement of the electron trigger which would certainly be part of the Level 2 system, but could be implemented in Level 1 if necessary, would be to require the electron to be isolated. This could be accomplished by requiring the energy in surrounding towers to be less than a certain fraction of E_{em} similar to the requirement of E_{had}.

As noted above, a unique crossing time can be associated with each electron trigger, and we assume that the results of the electron trigger for each crossing will be stored in a pipeline so that it can be combined with the information from other Level 1 trigger circuits for that crossing and also shipped to the Level 2 processors.

Muon Triggers Considerable attention was given to the topic of muon triggers.[4] Figure 13 shows estimated rates for all particles, particles with $p_t > 5$ GeV, particles exiting the calorimeter, and particles exiting the muon iron. For angles greater than 15°, simply the requirement that there exists a track segment pointing to the vertex will reduce the interaction associated rate to the level required, and should be sufficient to eliminate background from noise and cosmic rays. Should additional discrimination be required, a cut on the angle of the segment (at least in the central region) can be used to increase the momentum cut.

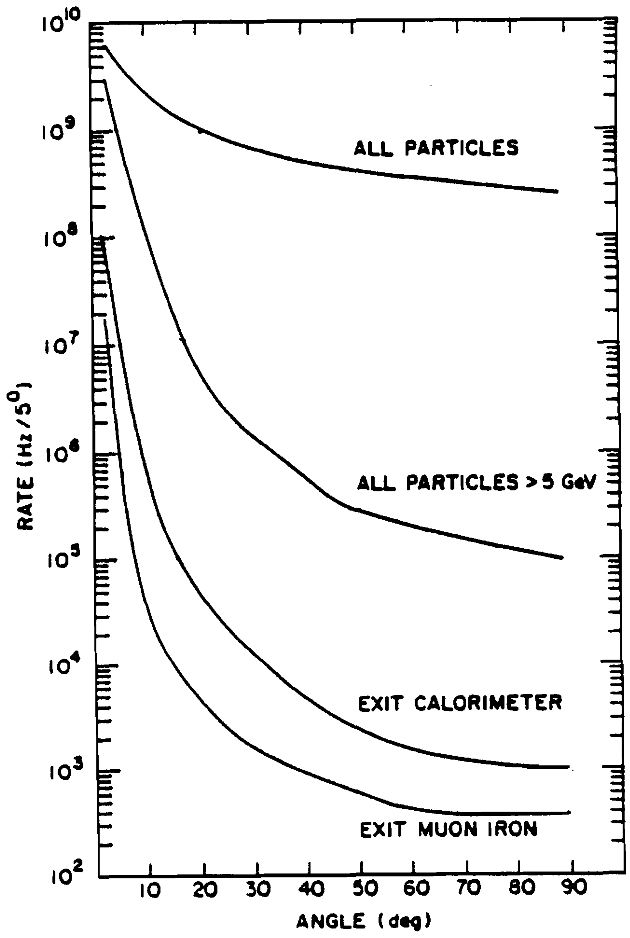

Figure 13
Estimated rates for all particles, particles with $P_t > 5$ GeV, particles exiting the calorimeter, and particles exiting the muon iron.

In the forward direction, the rate of muons (both prompt and from decays) is sufficiently large that a reasonably accurate determination of momentum will be required at Level 1; specifically, it will be necessary to impose a transverse momentum cut $p_t > 10\text{-}15$ GeV to reduce the trigger rate to acceptable levels. Since the displacement of a track from the infinite momentum trajectory for $p_t = 20$ GeV/c is small, e.g. 2.8 mm and 21 mm at polar angles of 0.77 and 5.7 degrees respectively, it will be necessary to use drift time information. A preliminary design of a track processor that performs a fast analog least-squares fit to the hit information was presented. The tower size corresponding to each track processor would be kept small enough to keep the rate in that trigger tower below 100 kHz in order to minimize ambiguities caused by multiple hits. To simplify the processor only hits from planes with low multiplicity would be utilized. A simulation of 1 TeV muons propagating in magnetically saturated iron was performed to study the effect of muon-induced electromagnetic showers; it was found that if five detector stations are used, each separated by 1 m steel, then at least three detector planes were clean for 97% of the events.

While further studies are clearly required, there was considerable optimism that it should be reasonably straightforward to design a muon Level 1 trigger which would reduce the trigger rate to less than 10 kHz.

Triggers for High P_t Tracks The challenge for tracking is sufficiently severe that to consider triggers on high p_t tracks at Level 1 might seem absurd. Nonetheless there was considerable optimism at the workshop that it should be possible to at least search for track *segments* with rather fast and simple circuits. Since it is likely that for the central track chamber the converted times will be stored on or near the chamber, with subsequent multiplexed readout, the track segment circuitry would also have to located there if a large fraction of the wires were to be utilized. Alternatively, signals from a subset of the wires, perhaps 5 - 10% could be brought out to a remote track processor.

Level 2 Triggers

The task for the Level 2 Triggers is to filter the 10,000 - 100,000 per second rate from Level 1 down to about 1000 per second appropriate to full digitization and processing by Level 3. This factor of 10 to 100 must be achieved in 10 - 30 μsec. This level of performance is similar to that required of several existing and planned detectors such as CDF, UA1, UA2 and Tristan. Thus, experience is being accumulated on the technology needed for Level 2 triggering, and the strategies implemented in it.

A number of approaches can be incorporated into the strategy adopted for the Level 2 trigger. Those envisioned at this time are:

1. Refinement of calorimetry clustering, and more accurate and selective application of the various thresholds on total E_t, missing E_t, and single-cluster parameters.[26]

2. Use of tracking information. Only the simplest track segment finders are envisioned at present for Level 1. The additional time available at Level 2 is needed for the more complex pattern recognition problem implicit in track finding.[30,31]

3. Correlations. As higher-level signatures such as hadron or electromagnetic clusters, muons and stiff tracks emerge from Level 1 and intermediate stages of Level 2, logical combinations can be required to emphasize certain physics objectives. Conservation of transverse momentum and isolation criteria can be applied.

4. Triggers originating from weak or malfunctioning areas of the detector can be identified and suppressed.

5. Three-dimensional spatial relationships can be sorted out by correlating $r - \phi$ data with $r - z$ data.

6. Data from subsystems with slower readout, not available for Level 1, can be incorporated into the trigger. Silicon-strip vertex detectors, which are deeply-embedded in the center of the detector, with stringent power limitations, may fall into this category.

As an example, the Fermilab Trigger Workshop considered a specific physics process, viz., $H^c \to WW \to e\nu q\bar{q}$) [13] By combining the Level 1 electron and jet signatures, or the electron and jet signatures along with the isolation criteria for the electron, the estimates are 200 to 600 per second. (They relied heavily on a transition radiation detector for further improvement to a rate of <10 Hz.)

An interesting strategy which may prove useful on the time scales appropriate for Level 2 triggers is that of data-driven architecture which is currently under developement for fixed target experiments at Brookhaven and Fermilab.[32]

DATA ACQUISITION AND LEVEL 3 TRIGGERING

Multiplexer-ADC-Buffers

When the Level 2 trigger requirements have been met by an event, the analog data must be digitized and all data moved out for software processing as quickly as possible. This stage of data acquisition has been confronted by a number of large colliding beams detectors already in operation, and their methods of solution, with appropriate parameters, appear reasonable for SSC.[26,28] A high degree of parallelism is essential. The detector channels must be divided into groups, each served by a multiplexer (Mux), analog or digital as needed, an ADC where needed, and a digital memory/buffer capable of storing several events worth of data for the group. Figure 1 symbolizes these functions as being combined in a single device, the Multiplexer-ADC-Buffer (MAB), but, as is the case with existing detectors, some functions can be separate and/or incorporated into the front end systems. On the upstream end, the parameters of this device will vary considerably, depending on which detector subsystem is being served. On the downstream end, they should all look alike to the Event Builder which follows.

There are a number of considerations which must be taken into account in the design of an MAB tailored to the needs of a particular detector subsystem.

1. Sparse data scanning. Analog or digital thresholds must be imposed to avoid reading out empty channels. The occupancy rate per channel is an important consideration in determining the number of channels served by each multiplexer. Typically, one expects an average occupancy of about 10%, but substantial fluctuations may occur because of physics-related correlations such as jets.

2. The ADC parameters can vary depending on the required resolution. The required performance appears to be avail-

able in existing devices. For example, one can now obtain a 14-bit ADC which operates at 1 Mz, and 8-bit FADC's at several hundred MHz. Other approaches which may be employed to provide reasonable resolution over a wide dynamic range are logarithmic ADC's, split scale devices, or the "floating-point" ADC which uses a programmed pre-amp to switch ranges.

3. Local intelligence. A microprocessor will be used on-board to perform local housekeeping and accounting tasks such as packing and labelling data for a given event, monitoring channel performance, responding to messages from a central data acquisition controller, and supervision of the I O controllers.
4. Buffer Memory. Memory must be multi-ported and organized so that input from the front end, packing operations, and output to the event builder can take place simultaneously. A word-size of 32 bits, byte-addressable, with 100 nsec or better read/write time will be needed.
5. Input/Output controllers must be capable of simultaneous and independent operation at appropriate speeds.

Figure 14 is a conceptual example of how such a system might be configured. A rough calculation can yield some idea of the number of MAB's needed. Assume one-million detector channels with an average occupancy of 10%, a Level 2 trigger rate of 1000 Hz, and an average ADC time of 0.5 microsecond. On average, an MAB could digitize 2,000 pieces of data in the 1 msec time available, and, thus, serve 20,000 channels. In practice, one needs at least a factor of two for fluctuations. Thus, 100 to 200 MAB's would serve. This is not very different from the number of similar devices at CDF.

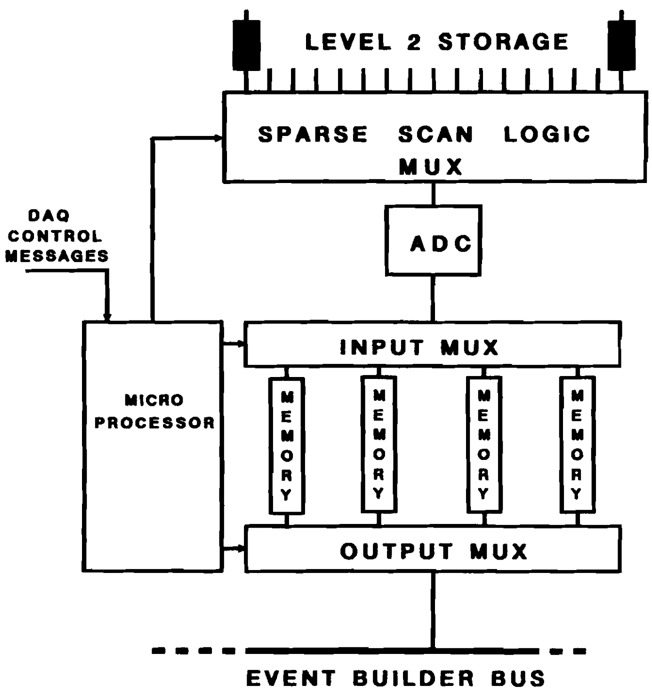

Figure 14
A block diagram of the Multiplexer-ADC-Buffer.

Event Builder

With as many as 1000 Level 2 triggers per second and as much as 1 MByte per event, the required data flow capability between the detector component electronics and the processor farm must be 1 GigaByte/sec. Clearly, a great deal of parallelism is needed, and experience in the required techniques is already being acquired in contemporary experiments. These large bandwidths can be handled by a manageable number of high-speed busses oerating in parallel into the "event builder" architecture illustrated in Fig. 1, or some similar architecture. As an example, twenty-five busses of 40 MByte capacity, similar to current Fastbus capabilities, would provide the needed bandwidth. Each bus would serve sequentially a number of Mux-ADC-Buffers from some portion of the detector. Data from a single event arriving in parallel on the busses (the vertical lines in Fig. 1) would be assembled in a set of dual-port memories along a single horizontal row in the event builder. At the completion of any of these parallel block transfers, the transmission of this data over a single high-speed bus to a common destination in the Level 3 processor farm can begin and continue until all the dual-port memories in the row have been processed.

All the basic ingredients for such a device are available or under construction (albeit on a smaller scale) for existing experiments.[33,34] An example is the CDF event builder,[35] implemented in Fastbus, which has two parallel input busses and a single output bus at present. Thus, it has the architecture appropriate to one row in the event builder matrix envisioned for SSC. Replicating it to provide more rows and columns is a fairly modest extension of its present design. (It also incorporates some of the features described in the previous section for memory buffers, local intelligence, and data reformatting.)

Level 3 Processor Farm

The Level 3 software data filter considered for SSC is a processor farm which must reduce an input trigger rate of 1000 Hz from Level 2 to a final rate of 1 Hz for data logging. It is also possible to envision variations on the farm architecture in which some of the processing power is upstream of or in the event builder in order to carry our some parts of the filter strategy for specific detector subsystems before all the data for an event is assembled in one place. The development of hardware for such devices is in a state of rapid change at this writing. Systems employing online microprocessor farms are already in use or under development, and 32-bit processors in non-farm architectures are performing specialized online data acquisition and filtering tasks. An example of the latter is the use of the Motorola 68020 in the muon trigger of UA1, which finds tracks in one dimension, combines tracks in space and applies trigger cuts.[26]

The fundamental idea of an "event-oriented" processor farm is to have a large number of single-board, 32-bit microprocessors, each equipped with an appropriately sized memory, and fully programmed to carry out the software filter strategy for an event using only its on-board resources. A host computer causes the data for an event to be downloaded into an idle processor and signals it to start its operation. When the task is complete, the processor signals that fact and the host computer initiates the appropriate response. For online operation, this would probably be to read a set of flags which summarize the response of the particular event to various data filtering tests, and then to decide whether or not to log the event to some storage medium. After this, the processor is returned to idle status, ready for another event.

Fermilab has developed a processor farm architecture called the Advanced Computer Program (ACP) which is now engaged in massive processing of offline data at a very favorable cost effectiveness ratio.[36] One major advantage of this system is that it is not limited to a single microprocessor. As new chips become available, new boards can be designed which meet the ACP specifications and take advantage of better microprocessors. Benchmark tests show the 68020 processors, using various mixtures of Fortran user code and assembly language library code, perform at 96% of a Vax-780, i.e. roughly 1 MIPS (million instructions per second). Preliminary tests on newer chips show improvements in speed of about a factor of five.

This architecture has been adapted for online use in CDF with the goal of an 80-processor farm in late 1987.[37] Hardware for 20 MByte/sec data transfers from Fastbus into farm memory is working, control programs for integrating the farm operations into the online envirnoment are under test, and software filtering algorithms are being written.

The parameters for a farm architecture serving an SSC detector were discussed in the Fermilab Trigger Workshop.[11,38–42] A crude approximation suggests that the number of computer cycles per second ought to scale at least as fast as the number of bytes per second emerging from the data acquisition system. The SSC to CDF bandwidth ratio of 1 Gigabyte/sec to 20 Megabytes/sec suggests that an SSC detector will need roughly 1000 processors operating at the 5 MIPS level. Experience gained in the near future should refine this estimate.

Additional Remarks

The discussion above centers on one particular architecture as an "existence proof" that the data handling tasks for an SSC detector are manageable. Alternatives and variations can be considered. For example, the farms might be some future generation of emulators similar in concept to the 168E and 3081E in present projects. The farm architecture could be varied considerably. The discussion above assumes that all the raw data from a single event is passed to a single processor. It is quite possible to envision a first tier of processors which occur in groups. Each member of the group receives only that part of the data for a specific subsystem in the detector and processes it. If all first-tier requirements are satisfied, then raw data and results from the several processors in this first tier can be transmitted to a single processor (with larger capacity and/or speed) in the next tier. Specialized co-processors become attractive candidates for this architecture. This architecture also implies an Event Builder architecture which differs in detail from that shown in Fig. 1, but the required technology is the same.

Even though the challenges of this part of the data acquisition system appears well addressed by existing technology and architectures, it is wide open for imaginative new constructions using the available building blocks.

SUMMARY

The Electronics and Triggering group at Snowmass-86 has produced conceptual designs for front-end electronics for calorimetry and central tracking in a 4π, SSC detector. These were judged to represent the most challenging electronics problems for such a detector. It appears that imaginative implementations of known technology can cope with the task.

However an aggressive R & D program will be required if one is to develop circuits, on an appropriate time scale, which fully exploit the capabilities of the state-of-the-art technology that is available today. A wide range of circuits will be required to encompass the variety of detectors used and the demands of both measurement and triggering. Areas of research and development of particular importance are:

1. Development of a complete drift chamber system-preamplifier, fast shaping amplifier, comparator, time-to--voltage or time-to-digital conversion, and analog or digital pipeline which meets the performance goals listed and consumes less than 100 mw. The goal is to locate the system on or near the chamber so that the number of cables required for readout is reduced by 10 – 100 from the number of channels. A variation of this system which measured charge would probably be suitable for TRD systems.
2. Further investigation of the fast pulse shaping, time resolution, and signal-to-noise that can be obtained with ionization calorimeters. This would include work on cold preamps, warm preamps, large capacitance FET's, protection systems, and pulse shaping amplifiers. Particular attention must be paid to the performance of the system as a whole-detector, cable, preamplifier, etc.
3. Development of analog memory units, using for example CCD's or switched capacitor techniques, which operate at 30 60 MHz and consume tens of mw per channel. The required dynamic range is likely to range from 7–8 bits for track chamber systems to 10–14 bits for calorimeter systems. The low power requirements will be more stringent for the track chamber systems than for the calorimeter.
4. Continued development of very low power, e.g. 1–5 mw per channel, charge preamplifiers including multiple sample-and-holds and multiplexing logic. The present generation of devices is probably not adequate for the high rates at SSC. Are substantially faster versions, without significant increase in power feasible?

The tasks of data acquisition and online processing also require a considerable work, though they appear to be logical extrapolations of sytems already in use or under development An early and well-supported R&D program is needed to confront the engineering questions associated with SSC electronics and triggering.

ACKNOWLEDGEMENTS

Needless to say a very large amount of effort is required to make a workshop such as this one a success. Lee Pondrom had the courage to take on the task of the overall organization. Special thanks to Joanne Day and her staff for their untiring efforts, both before and during the workshop, to make it happen and run smoothly. Robin Craven once again miraculously transformed empty condominiums into a productive computer center.

Special recognition goes to Veljko Radeka and Sergio Rescia for their valuable contributions to the workshop and for the many conversations we have had with them.

Finally we would like to thank Christine Feinberg for patiently preparing this report and Rene Donaldson for her efforts (and patience) in putting the entire Proceedings together.

References

1. H. H. Williams, "Detectors for the SSC: Summary Report", these Proceedings.
2. C. Baltay, J. Huston, and B. Pope. *Calorimetry for SSC Detectors,* these Proceedings.
3. D. G. Cassel and G. G. Hanson, *Report of the Central Tracking Group,* these Proceedings.
4. D. Carlsmith *et al., SSC Muon Detector Report,* these Proceedings.
5. P. Grannis *et al., Identification of Electrons at the SSC,* these Proceedings.
6. D. Theriot *et al., 4π Detectors,* these Proceedings.
7. Proceedings of the DPF Workshop on Collider Detectors: Present Capabilities and Future Possibilities, Lawrence Berkeley Laboratory, 1983, ed. Stewardt C. Loken and Peter Nemethy.
8. Proceedings of the Workshop on Triggering, Data Acquisition and Offline Computing for High Energy/High Luminosity Hadron-Hadron Colliders, November 11-14, 1985; B. Cox, R. Fenner and P. Hale, eds., Fermilab, Batavia, Illinois, (Trigger-85).
9. Proceedings of the ECFA-CERN Workshop on a Large Hadron Collider in the LEP Tunnel. CERN Report 84-10.
10. Proceedings of the 1984 Summer Study on the Design and Utilization of the Superconducting Super Collider; June 23 - July 13, 1984, Snowmass, Colorado; R. Donaldson and J. G. Morfin, eds; American Physical Society, New York, 1984, (Snowmass-84).
11. A. J. Lankford and G. P. Dubois, "Overview of Data Filtering/Acquisition for a 4π, Detector at the SSC," Trigger Workshop, ibid., p 185.
12. P. Cooper et al., "A Feasibility Design for the Readout of a 4π, SSC Detector", Trigger Workshop, ibid., p. 200.
13. M. Abolins et al., "Report of the High Level Trigger Group," Trigger Workshop, ibid., p 131.
14. P. Partridge, *Calorimeter Requirements for Tagging the Semileptonic Decays of Top Quarks,* Snowmass 84, 567. E. Fernandez *et al., Identification of W Pairs at the SSC,* Snowmass 84, 107.
15. V. Radeka, Academic Training Lectures at CERN. These lectures were also presented during the workshop.
16. NA34 Experiment, CERN.
17. A. Yamashita and K. Kondo, *Physics Noise to Calorimetry at SSC,* these Proceedings.
18. G. O. Alverson and J. Huston, *Estimation of Background Noise in LAr Detectors Due to Pileup,* these Proceedings.
19. G. M. Haller, D. R. Freytag, J. T. Walker, and S. I. Chae, IEEE Trans. Nucl. Sci. **NS-33**, 221 (1986); D. R. Freytag and J. T. Walker, IEEE Trans. Nucl. Sci. **NS-32**, 622 (1985).
20. G. Drake *et al.,* IEEE Trans. Nucl. Science **NS-33**, 893 (1986).
21. G. Hanson and D. Meyer, *Charged Particle Traking and Vertex Detection Group Summary Report,* Snowmass 84, p 585.
22. J. Fischer, A. Hirsoho, V. Radeka, P. Rehak, Nucl. Instrum. Methods, **A238**, 249 (1985).
23. B. Schmidt, Heidelberg Report, HD-PY/86/06.
24. Y. Arai and T. Ohsugi. *An Idea of Deadtimeless Readout System by Using Time Memory Cell,* these Proceedings.
25. P. Franzini et al., "Lowest Level Trigger for SSC General Purpose Detectors," Trigger-85, p. 93.
26. J. Dorenbosch, "Triggers in UA2 and UA1," Trigger-85, p. 134.
27. R. A. Rameika, "A Fast Analog Photon Trigger for Fermilab Experiment 705," Trigger Workshop, ibid., p 111.
28. D. Amidei et al., "The Trigger System for CDF", CDF Note 375, Fermilab, 1985; J. Hauser, "The CDF Level 2 Trigger Processor", CDF Note 446, Fermilab, 1986.
29. R. J. Wilson, "Electronic Trigger for the ASP Experiment," Trigger-85, p 118.
30. L. D. Gladney et al., "The CDF Track Processor - Prospects for the SSC," Trigger-85, p 152.
31. T. Ohsugi, "Fast Trigger Processor for Venus Detector of Tristan Experiment," Trigger-85, p 163.
32. W. Sippach, "Data Driven Architecture," Trigger-85, p 222.
33. The following CDF Notes from Fermilab describe various functions at the Multiplexer-ADC-Buffer level: T. Droege et al., "RABBIT System Specifications", CDF-119, 1983; F. Kirsten et al., "CDF Version of the SLAC Scanner Processor", CDF-312, 1985; C. Blocker, "MX Users Guide", CDF 315, 1985; G. Drake et al., "The RABBIT System", CDF-358, Fermilab, 1985.
34. M. Benetta et al., "The ALEPH Event Builder", CERN, 1985.
35. A.W. Booth et al., "Specifications for a Hardware Event Builder", CDF Note 452, Fermilab, 1986.
36. T. Nash et al., "The Fermilab Advanced Computer Program Multi- Microprocessor Project", Proceedings, Computing in High Energy Physics, Amsterdam (Netherlands), 1985.
37. J. T. Carroll, "Level 3 Filters at CDF," Trigger-85, p 254.
38. D. Cutts and C. van Ingen, "Modelling Microprocessor Farms for SSC Data Acquisition," Trigger-85, p 216.
39. L. R. Fortney, "Online Computer Farms - Configurations and Capabilities," Trigger-85, p 232.
40. D. Hedin, "Software Filter Strategies", Trigger-85, p 232.
41. T. Devlin, "Data Rates for Event Builders and Processor Farms", Trigger-85, p 232.
42. D. Cutts et al., "Data Acquisition and Filtering: Models and Software," Trigger-85, p 232.